Journal of Medicinal Chemistry

ACS Editors' Choice

Article

pubs.acs.org/jmc

Terms of Use

Development and Bioorthogonal Activation of Palladium-Labile Prodrugs of Gemcitabine

Jason T. Weiss,[†] John C. Dawson,[†] Craig Fraser,[†] Witold Rybski,[†,‡] Carmen Torres-Sánchez,[§] Mark Bradley,[∥] E. Elizabeth Patton,[†,‡] Neil O. Carragher,[†] and Asier Unciti-Broceta*[,†]

[†]Edinburgh Cancer Research UK Centre, and [‡]MRC Human Genetics Unit, MRC Institute of Genetics and Molecular Medicine, University of Edinburgh, Crewe Road South, Edinburgh EH4 2XR, U.K.

[§]Wolfson School of Mechanical and Manufacturing Engineering, Loughborough University, Loughborough LE11 3TU, U.K.

[∥]School of Chemistry, University of Edinburgh, West Mains Road, Edinburgh EH9 3JJ, U.K.

Supporting Information

ABSTRACT: Bioorthogonal chemistry has become one of the main driving forces in current chemical biology, inspiring the search for novel biocompatible chemospecific reactions for the past decade. Alongside the well-established labeling strategies that originated the bioorthogonal paradigm, we have recently proposed the use of heterogeneous palladium chemistry and bioorthogonal Pd^0-labile prodrugs to develop spatially targeted therapies. Herein, we report the generation of biologically inert precursors of cytotoxic gemcitabine by introducing Pd^0-cleavable groups in positions that are mechanistically relevant for gemcitabine's pharmacological activity. Cell viability studies in pancreatic cancer cells showed that carbamate functionalization of the 4-amino group of gemcitabine significantly reduced (>23-fold) the prodrugs' cytotoxicity. The *N*-propargyloxycarbonyl (*N*-Poc) promoiety displayed the highest sensitivity to heterogeneous palladium catalysis under biocompatible conditions, with a reaction half-life of less than 6 h. Zebrafish studies with allyl, propargyl, and benzyl carbamate-protected rhodamines confirmed *N*-Poc as the most suitable masking group for implementing *in vivo* bioorthogonal organometallic chemistry.

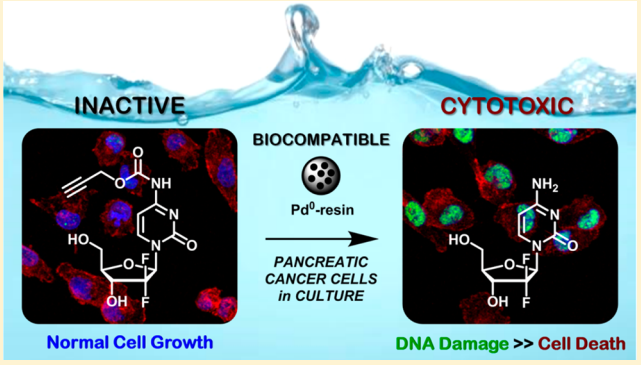

INTRODUCTION

Bioorthogonal chemistry is an emerging field of research that focuses on the development and application of selective chemical reactions susceptible to occurring in a biological environment without interfering with the normal function of its components.[1,2] These reactions are used as labeling methods to study cell constituents in their native state, including proteins and biomolecules that cannot be monitored by genetically encoded reporters (e.g., glycans, lipids, DNA, etc.).[1−4] Looking beyond the well-established labeling strategies that originated the bioorthogonal field, the induction of local chemotherapy by biologically inert means could allow for the reduction of adverse pharmacological effects in distant organs and tissues. This therapeutic paradigm has so far reached the clinic with the so-called photodynamic therapy, a method based on the local generation of cytotoxic reactive oxygen species by spatially controlled excitation (and subsequent energy transfer to the molecular oxygen present in the tissue) of a nontoxic systemically administered photosensitizer with a benign light source.[5] Following the same principle of bioorthogonality, novel strategies are being currently investigated by several groups to enable local conversion of chemically masked prodrugs into cytotoxic small molecules using either harmless electromagnetic radiations[6,7] or biocompatible heterogeneous catalysts.[8]

Technically speaking, for a bioorthogonal reaction to be optimal to living systems, the corresponding nonbiotic reactive partners need to display (i) high chemical stability to enzymatic processing and (ii) selective reciprocal reactivity in biocompatible conditions (water, pH 7.4, isotonicity, and 37 °C). Importantly, the reactants and the resulting product/s should be nontoxic, unless this is the intended outcome of the process. The Staudinger ligation and the copper-free azide alkyne cycloaddition, originally developed by the Bertozzi group,[9−11] are representative examples of such chemistry. In addition to catalyst-free ligations, the use of transition metals to functionalize biomolecules or activate fluorogenic probes in living cells has recently emerged as a new alternative in the field.[8,12,13] These biocompatible processes, also known as bioorthogonal organometallic (BOOM) reactions,[14] are mediated by nonbiotic transition metals such as copper(I),[15] ruthenium(II),[16−18] or palladium species[8,14,18−23] and have expanded

Received: April 3, 2014
Published: May 27, 2014

   dx.doi.org/10.1021/jm500531z | J. Med. Chem. 2014, 57, 5395−5404

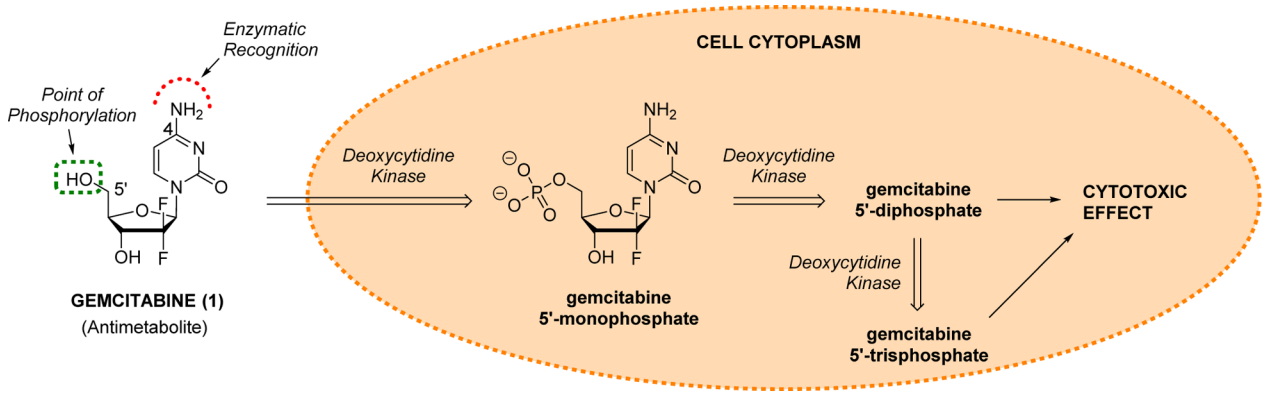

Figure 1. Gemcitabine and its cytotoxic mode of action. Following cell entry, gemcitabine is successively phosphorylated by deoxycytidine kinase at its 5′-OH position to generate cytotoxic metabolites.

Scheme 1. Synthesis of Gemcitabine Prodrugs[a]

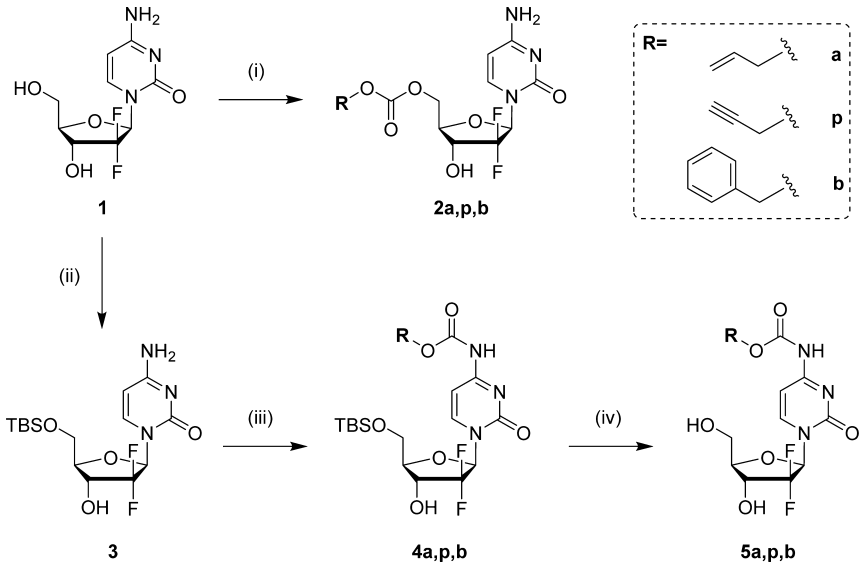

[a]Reagents and conditions: (i) DBU (2.5 equiv), DMF, addition of alkylchloroformate (1.5 equiv) at 4 °C, then r.t. overnight (47−53%); (ii) TBS-Cl (1.1 equiv), imidazole (3.5 equiv), DMF, r.t., 2.5 h (88%); (iii) pyridine (3.2 equiv), DMF or THF, addition of alkylchloroformate (1.5 equiv) at 4 °C, then r.t. overnight 12−48h (42−69%); (iv) TBAF (2.5 equiv), THF, r.t., overnight (62−92%).

the diversity of chemical groups and transformations suitable for use *bioorthogonally* in cell culture.

Aiming to modulate drug activity by an internal self-renewable control element rather than an external radiation source (e.g., light in photopharmacology[7]), we have recently proposed the development of nonbiological transition metals into biocompatible catalytic devices to allow the activation of systemically administered prodrugs at the location determined by the device.[8] This bioorthogonally activated chemotherapeutic strategy would be optimal to implement focalized treatment of unresectable primary or metastatic tumors and could also find application in the treatment of other disorders such as local infections, Parkinson's disease, cardiovascular disorders, etc. In the seminal investigation of such an approach,[8] we reported the development of a selective metallo-substrate (5-fluoro-1-propargyluracil) and a solid-phase palladium catalyst (Pd^0-resins) as a highly efficient bioorthogonal prodrug/activator system. On the basis of their complementary chemical roles, cytotoxic 5-fluorouracil was efficiently generated via extracellular BOOM catalysis in cell culture.[8] Importantly, when each of these reagents was cultured separately, neither of them exhibited cytotoxicity, demonstrating the feasibility of the method.

To explore this paradigm further, herein we report a comprehensive study on the development and evaluation of novel Pd^0-labile prodrugs of gemcitabine (deoxycytidine analogue clinically used to treat several types of cancers[24]) using two masking strategies: (i) carbonate formation at the 5′-OH group of the sugar moiety and (ii) carbamate masking of the 4-NH_2 group of the cytosine base (Figure 1).

RESULTS AND DISCUSSION

Design and Synthesis of Pd^0-Labile Gemcitabine Prodrugs. Gemcitabine (marketed as Gemzar by Eli Lilly and Co.) is an antimetabolite antineoplastic agent widely employed, in combination or alone, to treat several difficult-to-cure cancerous processes (e.g., nonsmall-cell lung carcinoma, metastatic breast cancer, and ovarian cancer),[24] including being a first-line therapy in the treatment of pancreatic cancer.[25] It displays a narrow therapeutic index, with its most severe side effects being myelosuppression, pulmonary toxicity, and renal failure.[24] Gemcitabine is intracellularly converted by deoxy-

dx.doi.org/10.1021/jm500531z | J. Med. Chem. 2014, 57, 5395−5404

cytidine kinase into its therapeutically active metabolites, the 5′-diphosphate and 5′-triphosphate derivatives (Figure 1). Gemcitabine 5′-diphosphate inhibits ribonucleotide reductase, a strictly conserved enzyme among all living organisms responsible for regulating the total rate of DNA synthesis, while the triphosphorylated derivative can become incorporated into the DNA, thereby inhibiting nuclear replication.[26]

On the basis of gemcitabine's mode of action, masking the 5′-OH group of its sugar moiety would chemically block the generation of its cytotoxic metabolites (Figure 1). In a different manner but similarly relevant, modification of the 4-amino group of the cytosine base would result in a reduction of the enzyme−substrate recognition. The absence of a free NH_2 group in that position would hinder the formation of essential hydrogen bonding interactions with the amino acid Asp133 located within the activation site of the enzyme, thus reducing the efficacy of the phosphorylation process.[27] Furthermore, the main detoxification route of gemcitabine is via hydrolytic deamination of the 4-NH_2 group. This is mediated in the liver by cytidine deaminase, which irreversibly converts gemcitabine into its inactive metabolite difluoro-deoxyuridine.[28] Consequently, masking the 4-NH_2 group would result in a doubly beneficial effect to the bioorthogonal strategy: it would reduce the cytotoxic properties of the resulting prodrug and protect the circulating drug precursor from premature liver deactivation before reaching the target tissue.

Allyl and propargyloxycarbonyl groups (Alloc and Poc, respectively) have been widely employed as OH and NH_2 protection strategies[29−32] and have shown sensitivity to palladium catalysis in biocompatible conditions.[8,14,19] Therefore, both groups were chosen to derivatize gemcitabine **1** into palladium-labile prodrugs. Because of the requirement of an additional hydrogen source to undergo palladium-mediated cleavage, the carboxybenzyl group (Cbz) was used to generate control prodrugs resistant to oxidative catalysis.[29,33] Prodrugs were synthesized using a semisynthetic strategy by functionalization of gemcitabine, **1** (Scheme 1). Treatment of **1** with allyl, propargyl, or benzyl chloroformate in the presence of DBU formed the corresponding carbonate prodrugs **2a,p,b** in moderate yields. To synthesize the 4-carbamate derivatives, the primary alcohol in position 5′ was first silylated using TBS-Cl and imidazole, followed by treatment with the corresponding alkyl chloroformates. TBAF-mediated deprotection yielded the final carbamate prodrugs **5a,p,b** in moderate to good yields.

Bioorthogonality Study: Carbonate vs Carbamate Gemcitabine Prodrugs. Although, in principle, the masking of either the 5′-OH or the 4-NH_2 group of gemcitabine could both have a significant impact on the drug's antiproliferative properties, the limiting factor in the development of any bioorthogonally activated prodrug approach is the stability of the protecting group to enzymatic metabolism. To determine the robustness of each deactivation strategy in cell culture, dose−response studies with gemcitabine (**1**) and prodrugs **2a,p,b** and **5a,p,b** were carried out in two human cancer cell lines. Pancreas adenocarcinoma BxPC-3 and Mia PaCa-2 cells were chosen as cell models due to the clinical relevance of gemcitabine as a first-line drug in pancreatic cancer therapy.[24,25] As shown in Figure 2, carbamate-protected prodrugs **5a,p,b** showed significant reduction of cytotoxicity relative to that of gemcitabine (EC_{50} (**5a,p,b**)/EC_{50} (**1**) > 23) in both cell lines, verifying the efficacy of the deactivation strategy. On the contrary, prodrugs **2a,p,b** displayed cytotoxicity similar to that of gemcitabine (**1**), suggesting that these prodrugs are rapidly

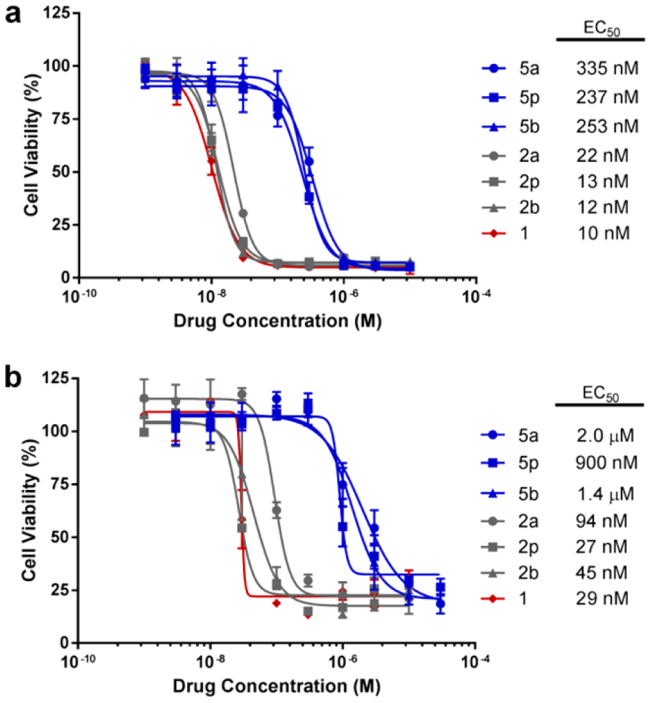

Figure 2. Study of the prodrugs' bioorthogonality. Semilog dose−response curves and calculated EC_{50} values of prodrugs **2a,p,b** (in gray) and **5a,p,b** (in blue) in comparison to those of unmodified gemcitabine (**1**, in red) in (a) BxPC-3 and (b) Mia PaCa-2 cells. Cell viability was measured at day 4 using PrestoBlue reagent. Error bars: ± SD from $n = 3$.

bioactivated inside cells. These results are in accordance with the weaker nature of the carbonate bond[32] and strongly indicate that carbonate-based masking strategies are not suitable for bioorthogonal applications. Consequently, only carbamate prodrugs **5a,p,b** were moved forward in this study.

Pd^0-Mediated Conversion of Prodrugs 5a,p,b into Gemcitabine. Polystyrene-supported reagents have been employed for a wide range of cell-based applications and have shown excellent biocompatibility both *in vitro* and *in vivo*.[8,34−36] As catalytically active Pd^0 nanoparticles can be readily generated and trapped in an amino-functionalized polystyrene matrix,[8,14] Pd^0-functionalized resins (150 μm in average diameter, Figure 3a) were prepared from NovaSyn TG amino resin HL following the procedure previously reported[8] and used as the heterogeneous palladium source (4.4% w/w in Pd). To test the susceptibility of the different carbamates to Pd^0-mediated catalysis in a biocompatible environment, compounds **5a,p,b** (100 μM) and Pd^0-resins (1 mg/mL, [Pd^0] = 400 μM) were dispersed in PBS (300 mOsm/kg, pH 7.4) and incubated at 37 °C for 24 h (Figure 3b). Reactions were analyzed by HPLC at different time points (0, 6, and 24 h), with prodrugs **5a,p,b** being retained for 2.56, 2.45, and 2.96 min, respectively, and the gemcitabine peak appearing at 0.93 min (Figure 3c−f). Treatment of Cbz-protected compound **5b** with the palladium source produced negligible levels of gemcitabine (**1**) after 24 h (Figure 3f), which corresponds with the need for an additional hydrogen source to achieve reductive cleavage of Cbz groups.[29,33] On the contrary, incubation of compounds **5a** and **5p** with Pd^0-resins led to the generation of significant levels of gemcitabine (**1**) in less than 24 h (Figure 3d,e). Interestingly, deprotection of **5p** proceeded in a faster and cleaner manner, with a reaction half-

dx.doi.org/10.1021/jm500531z | J. Med. Chem. 2014, 57, 5395−5404

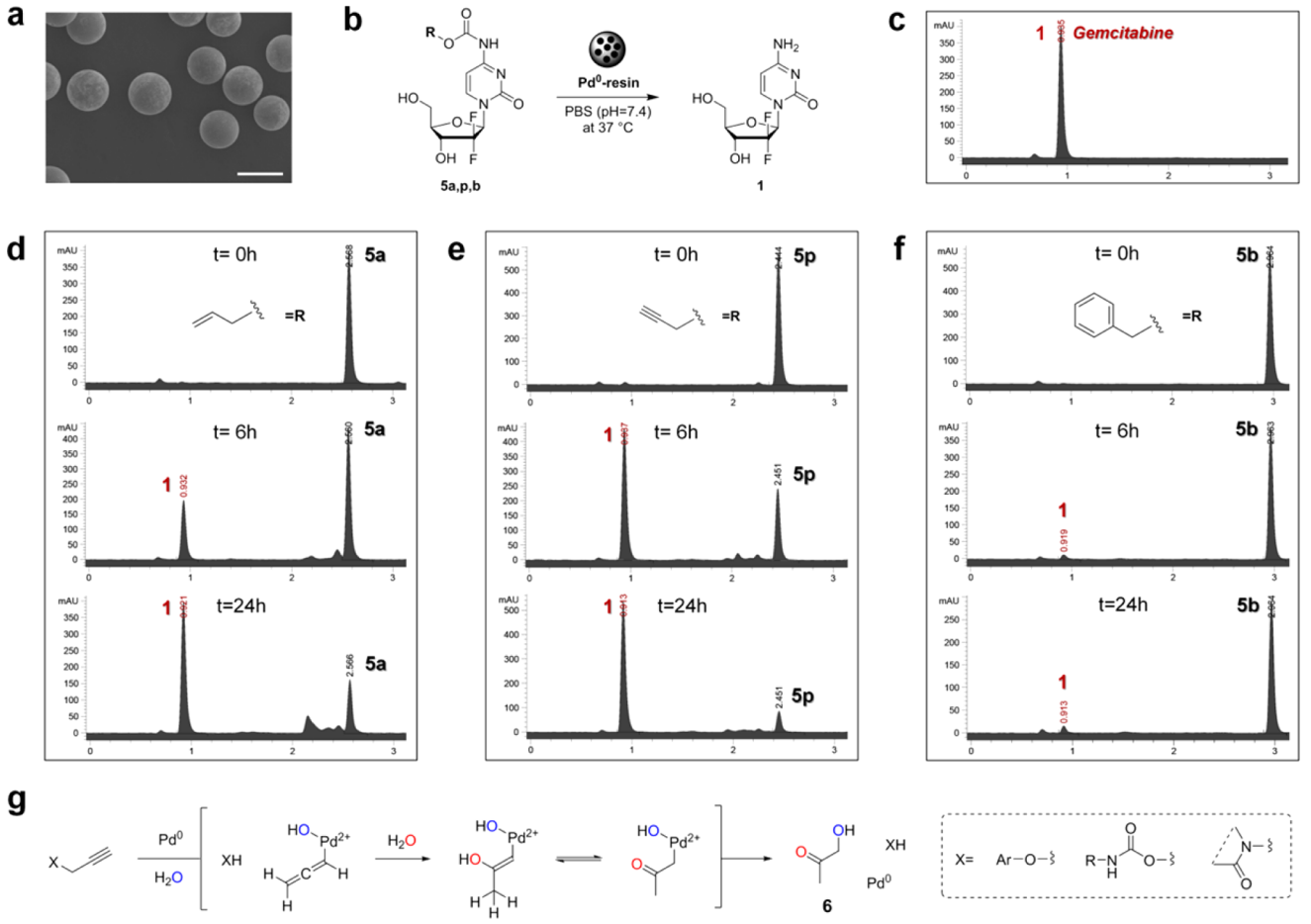

Figure 3. Palladium-mediated conversion assay in cell-free biocompatible conditions. (a) SEM image of Pd^0-resins. Scale bar = 150 μm. (b) Pd^0-mediated carbamate cleavage of compounds **5a,p,b**. (c) HPLC chromatogram of unmodified gemcitabine (**1**). (d–f) HPLC chromatograms (UV detector 280 nm) of 100 μM PBS solutions of compounds **5a** (left panel), **5p** (central panel), and **5b** (right panel) treated with Pd^0-resins at 37 °C for 0 h (top), 6 h (central), and 24 h (bottom). (g) Proposed mechanism for the Pd^0-catalyzed cleavage of *O*/*N*-propargyl groups in water.

life of <6 h (Figure 3e). These results are in accordance with previous observations[8,37,38] that have reported the efficient cleavage of various propargylated compounds by palladium species in biocompatible conditions. A potential mechanism for this process and for the reported formation of nontoxic 1-hydroxyacetone[8,39] (**6**) as a reaction byproduct is proposed in Figure 3g.

Pd^0-Mediated Prodrug Activation in Cell Culture. Bioorthogonal *in situ* generation of gemcitabine (**1**) from the carbamate prodrugs was first investigated in standard cell culture conditions with BxPC-3 cells using Pd^0-resins as the extracellular activating device. Prodrugs **5a,p,b** and Pd^0-resins were incubated independently (negative controls) or in combination (BOOM activation assay) and unmodified gemcitabine (**1**) used as the positive control. While neither the prodrugs nor the Pd^0-resins exhibited cytotoxicity, a combination of **5a** and **5p** with Pd^0-resins displayed a strong toxigenic effect (Figure 4), confirming the *in situ* bioorthogonal synthesis of cytotoxic gemcitabine (**1**). In the context of the present study, "toxigenic effect" describes the gemcitabine levels generated by each prodrug/Pd^0-resin combination in cell culture which in turn result in a cytotoxic phenotype. This effect is indirectly quantified by determining the antiproliferative activity caused by each prodrug/Pd^0-resin combination, which is directly proportional to the concentration of cytotoxic drug generated, and qualitatively proved by the verification of its mode of action. Consistent with the anticipated resistance of the *N*-Cbz functional group to palladium-mediated oxidative cleavage, cells treated with prodrug **5b** and Pd^0-resins did not produce any negative effect on cell viability.

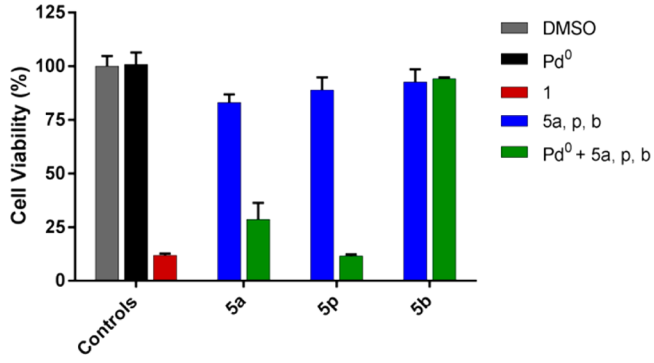

Figure 4. Palladium-mediated conversion of prodrugs **5a,p,b** into gemcitabine (**1**) in pancreatic cancer BxPC-3 cells. Experiments: 0.1% (v/v) DMSO (untreated cell control, in gray); 0.67 mg/mL of Pd^0-resins (negative control, in black); gemcitabine (100 nM, positive control, in red); prodrug **5a,p,b** (100 nM, negative control, in blue); and 0.67 mg/mL of Pd^0-resins + prodrug **5a,p,b** (100 nM, BOOM activation, in green). Cell viability was measured at day 5 using PrestoBlue reagent. Error bars: ± SD from n = 3.

dx.doi.org/10.1021/jm500531z | *J. Med. Chem.* 2014, 57, 5395–5404

Dose−response studies were subsequently carried out to compare the treatment of **5a** and **5p**/Pd^0-resin combinations at different concentrations in two cell lines: BxPC-3 and Mia PaCa-2 cells. As shown in Figure 5a,b, reduction of cell viability

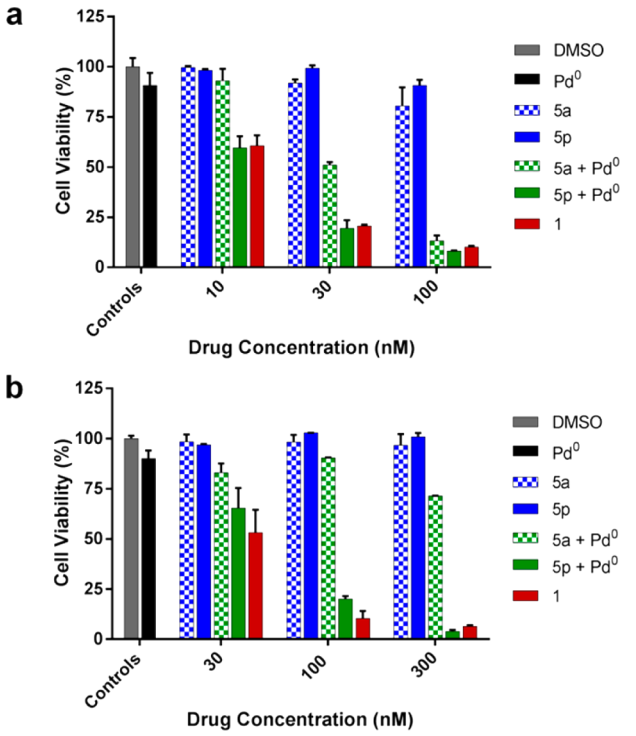

Figure 5. Bioorthogonally activated toxigenic effect in cancer cell culture: (a) BxPC-3 and (b) Mia PaCa-2 cells. Dose−response study: 0.1% (v/v) DMSO (untreated cell control, in gray); 0.67 mg/mL Pd^0-resins (negative control, in black); gemcitabine (positive control, in red); prodrug **5a,p** (negative control, in blue); and 0.67 mg/mL of Pd^0-resins + prodrug **5a,p** (BOOM activation, in green). Cell viability was measured at day 5 using PrestoBlue reagent. Error bars: ± SD from $n = 3$.

was observed with compounds **5a** and **5p** only when incubated with Pd^0-resins. Analysis of the toxigenic effect displayed by each prodrug/catalyst combination clearly ranked the *N*-Poc-protected prodrug **5p** as the most effective gemcitabine-generating precursor in the presence of Pd^0-resins, exhibiting analogous cytotoxic activity to that of the unmodified drug. Importantly, neither the palladium source nor the prodrugs exhibited antiproliferative activity when separately incubated at any of the concentrations tested, thus supporting the bioorthogonality of the strategy. It is important to note that the combination of *N*-Alloc-protected prodrug **5a** and Pd^0-resins resulted in significantly higher toxigenic effect against BxPC-3 cells than that in Mia PaCa-2 cells. Since both cell lines display similar sensitivity to unmodified gemcitabine, these results show that the palladium-mediated cleavage of the *N*-Alloc group of prodrug **5a** is significantly affected by either the cell type or the culture conditions (BxPC-3 cells are grown in RPMI, while Mia PaCa-2 cells are cultured in DMEM medium). On the contrary, the combined treatment of **5p** and Pd^0-resins displayed comparable toxigenic effects in both cell lines, indicating that the biological environment has little or no influence on the *N*-Poc deprotection process, as would be expected from a truly bioorthogonal reaction.

Real-time monitoring of BxPC-3 cell proliferation using an IncuCyte ZOOM microscope was performed to compare the effect of each prodrug/catalyst combination upon the kinetics of tumor cell growth. Time-lapse imaging of the negative controls **5a** and **5p** showed a standard growth curve up to 100% cell confluence level by day 4−5 (light and dark blue curves, respectively; Figure 6), while gemcitabine treatment efficiently

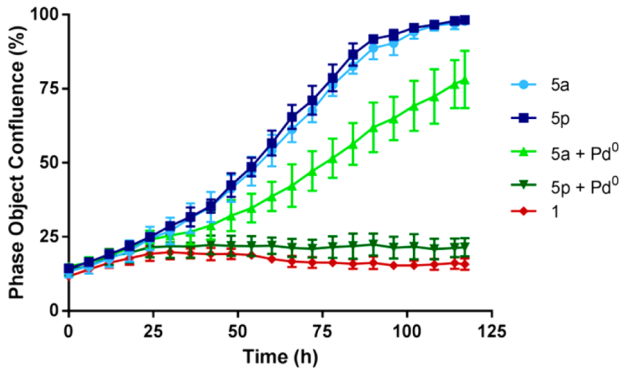

Figure 6. Real-time cell confluence study in pancreatic cancer BxPC-3 cells. The cell population was monitored for 120 h using an IncuCyte ZOOM system in an incubator (5% CO_2 and 37 °C). Drug/prodrug concentration: 30 nM. Error bars: ± SD from $n = 3$.

suppressed cell proliferation within 24 h. In accordance with the cell viability studies, the toxigenic effect mediated by either prodrug **5a** or **5p** incubated with Pd^0-resins (light and dark green curves, respectively; Figure 6) were patently different (see Supporting Information for a motion picture of the IncuCyte experiment). The prodrug **5p**/catalyst combination inhibited cell proliferation with the same efficacy and kinetic response as unmodified gemcitabine (**1**), proving that cytotoxic levels of the drug were rapidly generated. Although treatment with the **5a**/catalyst combination markedly delayed BxPC-3 cell growth relative to the negative controls, its antiproliferative effect was significantly inferior to either the **5p**/Pd^0-resins combination or unmodified gemcitabine (**1**), indicating quantitatively lower levels of active drug being generated.

Study of Cytotoxic Mode of Action. Double-stranded breaks caused by DNA damage induce phosphorylation of the variant histone of the H2A protein family, γ-H2AX. Phosphorylated γ-H2AX is responsible for recruiting and localizing the DNA repair mechanism.[40] Gemcitabine damages DNA through partial DNA chain termination and by stalling of replication forks.[41] In order to analyze the toxigenic effect caused by the prodrug/catalyst combination at the molecular level, immunofluorescence studies were carried out to probe for phosphorylated γ-H2AX as a marker of DNA damage in Mia PaCa-2 cells (Figure 7). While the negative controls (Pd^0-resins or prodrug **5p** separately incubated; Figure 7a,b) did not show the presence of phosphorylated γ-H2AX in the cell nuclei, cells treated with either gemcitabine (Figure 7c) or the Pd^0-resins + **5p** combination (Figure 7d) expressed significant levels of phospho-γ-H2AX. This study further illustrates that the cytotoxic activity generated from the prodrug/catalyst combination and unmodified gemcitabine is equivalent.

Pd^0-Mediated Probe Activation in Zebrafish. We have recently shown that catalytically functional Pd^0-resins can be implanted in the yolk sac of zebrafish embryos without inducing toxicity or affecting the embryo development.[8] To compare the *in vivo* bioorthogonality and palladium sensitivity

dx.doi.org/10.1021/jm500531z | J. Med. Chem. 2014, 57, 5395−5404

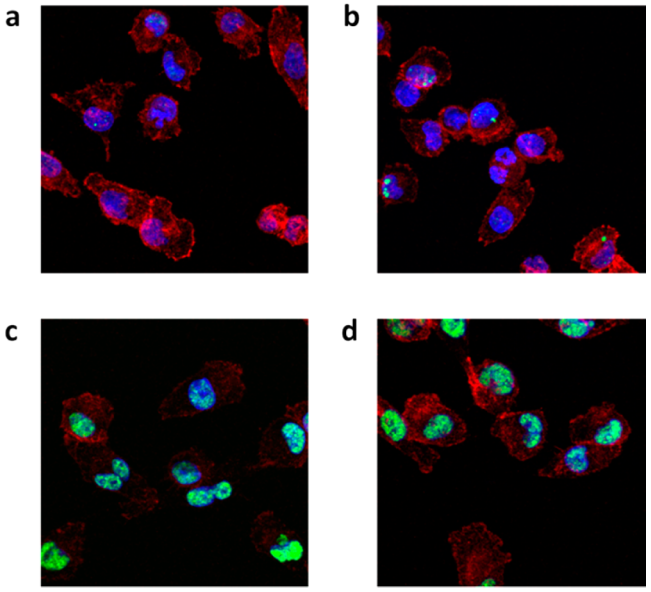

Figure 7. DNA damage study. Merge fluorescent images of Mia PaCa-2 cells 24 h after treatment with (a) 0.67 mg/mL Pd^0-resins (negative control); (b) prodrug **5p** (300 nM, negative control); (c) gemcitabine (300 nM, positive control); and 0.67 mg/mL of Pd^0-resins + prodrug **5p** (300 nM, BOOM activation assay). Fluorescent labels: Hoechst 33342 for cell nuclei (blue), Alexa Fluor 594 phalloidin for F-actin (red), and anti-phospho-histone γ-H2AX + Alexa Fluor 488 secondary antibody for phosphorylated γ-H2AX (green).

of each of the carbamate protecting groups under study, *N*,*N*′-bis(alkyloxycarbonyl) rhodamine derivatives **8a,p,b** were prepared and used as off-on fluorescent probes (Figure 8a). Compounds **8a,p,b** were synthesized from rhodamine 110, **7**, by reaction with the corresponding alkylchloroformate and a base (triethylamine or pyridine) in dry DMF. The resulting nonfluorescent rhodamine precursors were incubated with 2-dpf zebrafish embryos containing either a nonfunctionalized resin (nonactive resin) or a Pd^0-resin (active) in the yolk sac for 24 h and subsequently analyzed by fluorescence microscopy. Zebrafish embryos treated with Alloc-protected compound **8a** showed high levels of fluorescence emission regardless of the presence or absence of palladium, particularly from the yolk sac and the digestive system (Figure 8b,c, top panel). Because of the high levels of biochemically generated fluorescence background, local palladium-mediated activation of **8a** within the zebrafish yolk was not detectable, an indication of the low bioorthogonality of the *N*-Alloc group in zebrafish. On the contrary, compounds **8p** and **8b** showed improved biochemical stability, with the fluorescent background signal mostly being observed from the digestive system, which is in accordance with our previous observations.[8] As expected, Cbz-protected compound **8b** did not exhibit sensitivity to palladium catalysis (Figure 8b,c, lower panel), while local palladium-mediated generation of rhodamine 110 was clearly observed from **8p** in the zebrafish yolk sac containing a Pd^0-resin (Figure 8b,c, middle panel). As shown in Figure 8d, image analysis demonstrated up to a 4-fold increase in fluorescence intensity within close vicinity of the Pd^0-resin (blue line). On the contrary, apart from the autofluorescence intensity typically observed from the nonfunctionalized resin, this inactive resin did not lead to an increment of fluorescence levels in the area surrounding it (red line). This study suggests that, from the carbamate groups herein studied, only the *N*-Poc masking strategy would allow generating locally increased concentrations of a functionally active small molecule by palladium heterogeneous catalysis *in vivo*.

CONCLUSIONS

The chemical protection of gemcitabine's 4-amino group as a carbamate led to a significant reduction of the drug's cytotoxic activity. Among the carbamate derivatives investigated, the *N*-Poc group exhibited the highest sensitivity to palladium-mediated cleavage at 37 °C in both buffered solution and cell culture. This is noteworthy since, to date, our group[14,19] and others[12,13,16−18,42−44] have favored the use of *N*-Alloc groups over *N*-Poc to implement coupling and decoupling strategies[45] for BOOM studies. Cell viability, time-lapse microscopy, and DNA damage assays confirmed the bioorthogonal generation of cytotoxic gemcitabine from the combined treatment of extracellular Pd^0-resins and the *N*-Poc-protected precursor in pancreatic cancer cell culture. Unlike the *N*-Alloc- and *N*-Cbz-protected derivatives, the bis-*N*,*N*′-Poc-rhodamine 110[8] became locally activated by a Pd^0-resin implanted in the yolk sac of zebrafish embryos, further reinforcing its nomination as the carbamate group of choice for developing bioorthogonal studies based on heterogeneous palladium catalysis. Parallel independent studies from Chen et al. (intracellular protein activation by palladium-mediated homogeneous catalysis), published just before the submission of this article,[46] reported analogous findings with the *N*-Poc group. Finally, the simplicity of the masking strategy together with the biocompatibility and efficacy of the palladium-mediated deprotection process underlines the potential of this method to modulate the pharmacodynamics and pharmacokinetics of amino-containing drugs.

EXPERIMENTAL PROCEDURES

Synthetic Procedures. *General Methods.* Chemicals and solvents were purchased from Fisher Scientific, Sigma-Aldrich, or VWR International Ltd. Gemcitabine HCl was purchased from Shandong Boyuan Pharmaceutical Co. Ltd. NMR spectra were recorded at ambient temperature on a 500 MHz Bruker Avance III spectrometer. Chemical shifts are reported in parts per million (ppm) relative to the solvent peak. R_f values were determined on Merck TLC Silica gel 60 F254 plates under a 254 nm UV source. Purification was carried out by flash column chromatography using commercially available silica gel (220−440 mesh, Sigma-Aldrich). All compounds used in the biological experiments were >95% pure, as measured by HPLC using an evaporative light scattering detector. Method: eluent A, water and formic acid (0.1%); eluent B, acetonitrile and formic acid (0.1%); A/B = 95:5 to 5:95 in 3 min, isocratic 1 min, 5:95 to 95:5 in 1 min, and isocratic 1 min.

Synthesis of Pd^0-Resins. Pd^0-functionalized resins were prepared from NovaSyn TG amino resin HL (0.39 mmol NH_2/g) as previously described.[8]

*Synthesis of Carbonate-Protected Derivatives **2a,p,b**.* Gemcitabine HCl (150 mg, 0.5 mmol) was dissolved in dry DMF (3 mL) with DBU (194 μL, 1.30 mmol) under N_2 atmosphere. The mixture was then cooled to 4 °C in an ice bath. Allyl, propargyl, or benzyl chloroformate (0.75 mmol) was added dropwise to the mixture. The mixture was stirred overnight and allowed to warm up to room temperature (r.t.). The solvents were then removed *in vacuo*, the crude redissolved with 25% isopropanol (IPA) in $CHCl_3$ (20 mL), and washed with H_2O (20 mL). The aqueous layer was washed with 25% IPA in $CHCl_3$ (3 × 20 mL) and the combined organic layers dried over $MgSO_4$, filtered, and concentrated *in vacuo*.

*4-Amino-1-(2-deoxy-2,2-difluoro-5-O-[allyloxycarbon-yl]-β-D-erythro-pentofuranosyl)pyrimidin-2(1H)-one] (**2a**).* The crude was purified by column chromatography using 8% MeOH in DCM (R_f

dx.doi.org/10.1021/jm500531z | J. Med. Chem. 2014, 57, 5395−5404

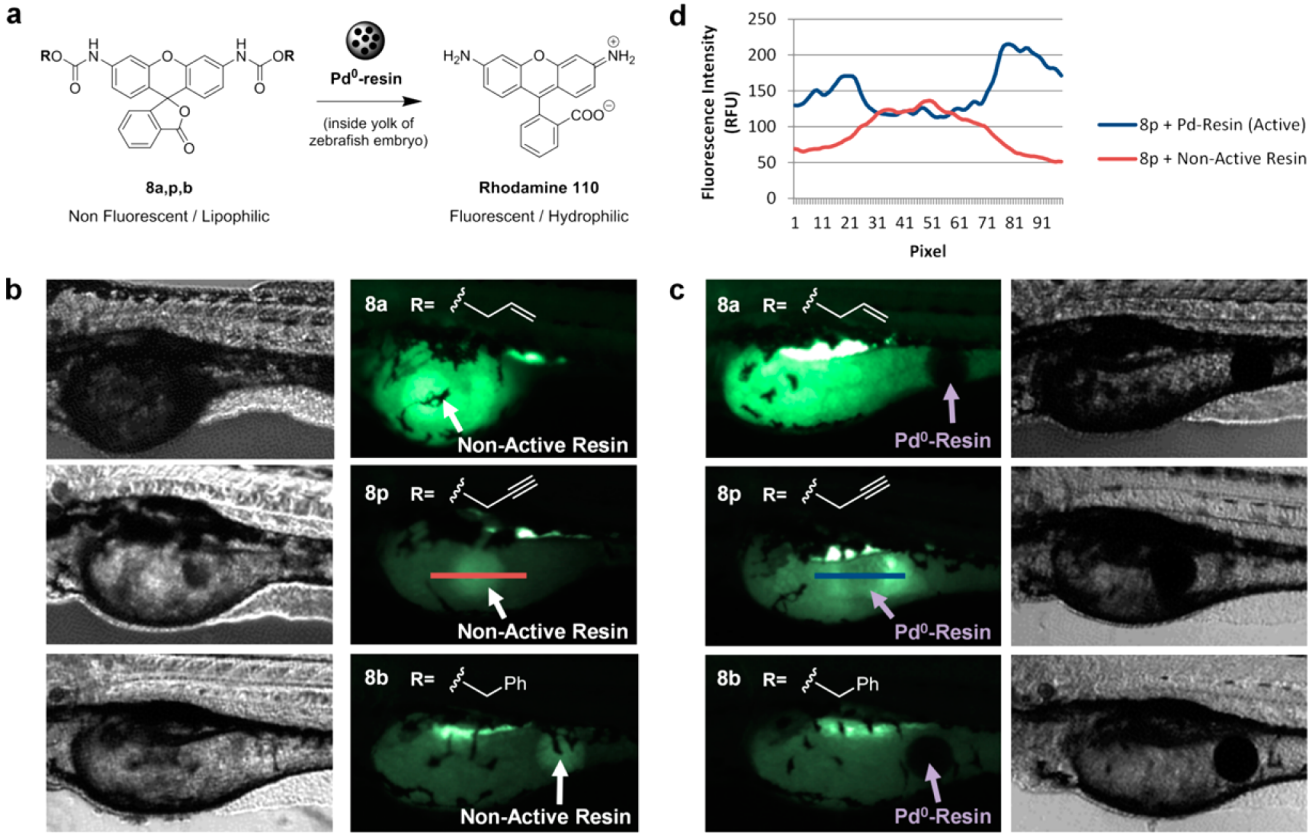

Figure 8. Pd^0-mediated carbamate cleavage of rhodamine precursors in zebrafish. (a) BOOM conversion of nonfluorescent lipophilic compounds **8a,p,b** into highly fluorescent hydrophilic rhodamine 110. (b) 3-dpf zebrafish embryos (n = 5) containing a nonfunctionalized resin (indicated with white arrows) after incubation with 5 μM of compounds **8a** (top), **8p** (middle), and **8b** (bottom) for 24 h at 31 °C. (c) 3-dpf zebrafish embryos (n = 5) containing a Pd^0-resin (indicated with purple arrows) after incubation with 5 μM of compounds **8a** (top), **8p** (middle), and **8b** (bottom) for 24 h at 31 °C. Fish were imaged by phase contrast and fluorescent microscopy (ex., 470/40; em., 525/50). (d) Analysis of fluorescence intensity/pixel across a horizontal line of approximately 300 μm drawn in the yolk sac of the zebrafish embryos and encompassing both the resin and the area surrounding it. Note: the red and blue lines represent the areas of fluorescence intensity profile measured over the inactive resin (b, middle right panel) and the Pd^0-resin (c, middle left panel), respectively.

0.29, 10% MeOH in DCM), which yielded a light green solid (90 mg, 52% yield). ^{1}H NMR (500 MHz, DMSO) δ 7.50 (d, J = 7.5, 1H), 7.42 (d, J = 5.7, 2H), 6.44 (d, J = 6.3, 1H), 6.17 (s, 1H), 5.99−5.89 (m, 1H), 5.79 (d, J = 7.5, 1H), 5.38−5.23 (m, 2H), 4.63 (dt, J = 5.5, 1.3, 2H), 4.47−4.37 (m, 2H), 4.18 (s, 1H), 4.07−4.00 (m, 1H). ^{13}C NMR (126 MHz, DMSO) δ 165.63 (C), 154.48 (C), 154.07 (C), 141.16 (CH), 132.02 (CH), 122.60 (t, J_{C-F} = 264.6, C), 118.56 (CH_2), 94.87 (CH), 83.89 (CH), 77.22 (CH), 70.09 (t, J_{C-F} = 25.2, CH), 68.16 (CH_2), 66.31 (CH_2). LRMS (ESI) m/z 346.0 $[M - H]^-$. HRMS (FAB) m/z $[M - H]^-$ calcd for $C_{13}H_{14}O_6N_3F_2$, 346.0856; found, 346.0859.

*4-Amino-1-(2-deoxy-2,2-difluoro-5-O-[propargyloxy-carbonyl]-β-D-erythro-pentofuranosyl)pyrimidin-2(1H)-one] (**2p**).* The crude was purified by column chromatography using 8% MeOH in DCM (R_f 0.23, 10% MeOH in DCM), which yielded a pale yellow solid (81 mg, 47%). ^{1}H NMR (500 MHz, DMSO) δ 7.65 (d, J = 7.5, 1H), 7.44 (d, J = 13.0, 2H), 6.24 (t, J = 5.0, 1H), 5.81 (d, J = 7.5, 1H), 5.28−5.26 (m, 2H), 4.88 (s, 2H), 4.22−4.16 (m, 1H), 3.79−3.62 (m, 3H). ^{13}C NMR (126 MHz, DMSO) δ 165.71 (C), 154.41 (C), 152.63 (C), 141.43 (CH), 121.48 (t, J_{C-F} = 262.1, C), 94.83 (CH), 83.76 (CH), 79.16 (CH), 78.11 (CH), 77.25 (C), 73.39 (t, J_{C-F} = 26.5, CH), 59.18 (CH_2), 56.37 (CH_2). LRMS (ESI) m/z 379.9 $[M + Cl]^-$. HRMS (FAB) m/z $[M - H]^-$ calcd for $C_{13}H_{12}O_6N_3F_2$, 344.0700; found, 344.0728.

*4-Amino-1-(2-deoxy-2,2-difluoro-5-O-[benzyloxy-carbonyl]-β-D-erythro-pentofuranosyl)pyrimidin-2(1H)-one] (**2b**).* The crude was purified by column chromatography using 6% MeOH in DCM (R_f 0.05, 4% MeOH in DCM), which yielded a white solid (70 mg, 53% yield). ^{1}H NMR (500 MHz, DMSO) δ 7.49 (d, J = 7.5, 1H), 7.44−7.33 (m, 7H), 6.44 (d, J = 6.2, 1H), 6.17 (s, 1H), 5.76 (d, J = 7.5, 1H), 5.17 (s, 2H), 4.52−4.35 (m, 2H), 4.18 (s, 1H), 4.03 (t, J = 6.1, 1H). ^{13}C NMR (126 MHz, DMSO) δ 165.60 (C), 154.45 (C), 154.20 (C), 141.15 (CH), 135.04 (C), 128.50 $(CH)_2$, 128.42 (CH), 128.17 $(CH)_2$, 122.57 (t, J_{C-F} = 258.3, C), 94.83 (CH), 83.86 (CH), 77.18 (CH), 70.10 (t, J_{C-F} = 23.4, CH), 69.22 (CH_2), 66.39 (CH_2). LRMS (ESI) m/z 398.0 $[M + H]^+$. HRMS (FAB) m/z $[M - H]^-$ calcd for $C_{17}H_{16}O_6N_3F_2$, 396.1013; found, 396.1016.

*Synthesis of Carbamate-Protected Derivatives **5a,p,b**. Synthesis of Silylated Derivative **3**.* Gemcitabine HCl (500 mg, 1.67 mmol) was dissolved in dry DMF (5 mL) with imidazole (398 mg, 5.85 mmol) and TBS-Cl (301 mg, 2.0 mmol) stirred at r.t. overnight. The mixture was then concentrated *in vacuo*, redissolved in EtOAc (50 mL), and washed with H_2O (50 mL). The aqueous layer was washed twice with EtOAc and, subsequently, the organic layers combined, washed with brine (150 mL), and dried over $MgSO_4$. The crude was purified by column chromatography (eluent 8% MeOH in DCM) to yield intermediate **3** as a white solid 552 mg (88%). ^{1}H NMR (500 MHz, DMSO) δ 7.63 (d, J = 7.5, 1H), 7.38 (s, 2H), 6.31 (d, J = 5.1, 1H), 6.14 (t, J = 7.7, 1H), 5.76 (d, J = 7.5, 1H), 4.19−4.06 (m, 1H), 3.95 (d, J = 11.8, 1H), 3.90−3.77 (m, 2H), 0.90 (s, 9H), 0.09 (d, J = 2.1, 6H). ^{13}C NMR (126 MHz, DMSO) δ 165.58 (C), 154.56 (C), 139.91 (CH), 122.95 (t, J_{C-F} = 258.3, C), 94.51 (CH), 83.45 (t, J_{C-F} = 31.5, CH), 79.76 (CH), 68.23 (t, J_{C-F} = 22.7, CH), 60.72 (CH_2), 25.71 (CH_3), 17.99 (C), −5.52$(CH_3)_3$, −5.63 $(CH_3)_2$. MS (ESI) m/z 378.0 $[M + H]^+$.

dx.doi.org/10.1021/jm500531z | J. Med. Chem. 2014, 57, 5395−5404

Synthesis of Intermediate ***4a***. Compound **3** (100 mg, 0.27 mmol) was dissolved in dry THF (2.5 mL) with pyridine (61 μL, 0.75 mmol) and the mixture cooled to 4 °C in an ice bath. Allyl chloroformate (55 μL, 0.52 mmol) was added dropwise to the mixture and stirred for 1 h. The solvent was removed *in vacuo* and purified via flash chromatography (eluent: 3% MeOH in DCM) to yield compound **4a** as a white solid.

*4-(Allyloxycarbonylamino)-1-(2-deoxy-2,2-difluoro-5-O-[tert-butyl(dimethyl)silyl]-β-D-erythro-pentofuranosyl)pyrimidin-2(1H)-one] (**4a**)*. Eighty-three milligrams, 69% yield (R_f 0.53, 10% MeOH in DCM). ^{1}H NMR (500 MHz, MeOD) δ 8.29 (d, *J* = 7.7, 1H), 7.32 (d, *J* = 7.6, 1H), 6.25 (t, *J* = 6.7, 1H), 6.04−5.94 (m, 1H), 5.39 (dq, *J* = 17.2, 1.5, 1H), 5.27 (dq, *J* = 10.5, 2.6, 1.3, 1H), 4.70 (dt, *J* = 5.6, 1.4, 2H), 4.33−4.24 (m, *J* = 12.5, 8.8, 1H), 4.10 (d, *J* = 12.0, 1H), 4.03−3.89 (m, 2H), 0.97 (s, 9H), 0.17 (s, 6H). ^{13}C NMR (126 MHz, MeOD) δ 165.38 (C), 157.33 (C), 154.35 (C), 144.81 (CH), 133.24 (CH), 123.87 (t, J_{C-F} = 259.7, C), 118.88 (CH_2), 96.95 (CH), 86.22 (t, J_{C-F} = 32.8, CH), 82.46 (CH), 69.56 (t, J_{C-F} = 23.9, CH), 67.56 (CH_2), 61.68 (CH_2), 26.37 (CH_3)$_3$, 19.26 (C), −5.35 (CH_3), −5.45 (CH_3). MS (ESI) *m*/*z* 462.0 $[M + H]^+$.

Synthesis of Intermediates ***4p,b***. Compound **3** (100 mg, 0.27 mmol) was dissolved in dry DMF (2.5 mL) with pyridine (61 μL, 0.75 mmol) and the mixture cooled to 4 °C in an ice bath. Propargyl (63 μL, 0.65 mmol) or benzyl chloroformate (56 μL, 0.39 mmol) was added dropwise to the mixture. The mixture was stirred at r.t. overnight (for **4b**) or for 48 h (for **4p**). The solvents were removed and the mixture redissolved with EtOAc (30 mL) and washed with H_2O (30 mL). The aqueous layer was washed twice more with EtOAc (30 mL each) and the combined organic layers dried over $MgSO_4$, solids filtered off, and concentrated *in vacuo*. The crude was purified via flash chromatography (eluent: 3% MeOH in DCM) to yield compounds **4p,b** as white solids.

*4-(Propargyloxycarbonylamino)-1-(2-deoxy-2,2-difluoro-5-O-[tert-butyl(dimethyl)silyl]-β-D-erythro-pentofuranosyl)pyrimidin-2(1H)-one] (**4p**)*. Fifty-three milligrams, 44% yield. (R_f 0.6, 10% MeOH in DCM) ^{1}H NMR (500 MHz, MeOD) δ 8.30 (d, *J* = 7.6, 1H), 7.29 (d, *J* = 7.6, 1H), 6.25 (t, *J* = 6.7, 1H), 4.84 (d, *J* = 2.5, 2H), 4.33−4.24 (m, 1H), 4.10 (d, *J* = 12.0, 1H), 4.03−3.90 (m, 2H), 2.99 (t, *J* = 2.3, 1H), 0.98 (s, 9H), 0.17 (s, 6H). ^{13}C NMR (126 MHz, MeOD) δ 165.28 (C), 157.29 (C), 154.57 (C), 144.97 (CH), 123.88 (t, J_{C-F} = 259.6, C), 96.93 (CH), 86.15 (t, J_{C-F} = 32.8, CH), 82.49 (CH), 77.70 (C), 76.92 (CH), 69.57 (t, J_{C-F} = 22.7, CH), 61.69 (CH_2), 54.34 (CH_2), 26.36 (CH_3)$_3$, 19.26 (C), −5.36 (CH_3), −5.46 (CH_3). MS (ESI) *m*/*z* 460.2 $[M + H]^+$.

*4-(Benzyloxycarbonylamino)-1-(2-deoxy-2,2-difluoro-5-O-[tert-butyl(dimethyl)silyl]-β-D-erythro-pentofuranosyl)pyrimidin-2(1H)-one] (**4b**)*. Fifty-six milligrams, 42% yield (R_f 0.5, 10% MeOH in DCM) which. ^{1}H NMR (500 MHz, CDCl3) δ 8.11 (d, *J* = 7.5, 1H), 7.40−7.32 (m, 5H), 7.25−7.20 (m, 1H), 6.40−6.32 (m, 1H), 5.22 (s, 2H), 4.41−4.31 (m, 1H), 4.09−3.85 (m, 3H), 0.93 (s, 9H), 0.12 (s, 6H). ^{13}C NMR (126 MHz, DMSO) δ 162.90 (C), 154.93 (C), 152.35 (C), 144.42 (CH), 135.02 (C), 128.85 (CH_2), 128.43 (CH_2), 122.32 (t, J_{C-F} = 258.3, C), 95.54 (CH), 84.56 (t, J_{C-F} = 32.8, CH), 81.62 (CH), 69.31 (t, J_{C-F} = 26.5, CH), 68.22 (CH_2), 60.69 (CH_2), 25.97 (CH_3)$_3$, 18.5 (C), −5.32 (CH_3), −5.41 (CH_3). MS (ESI) *m*/*z* 534.1 $[M + Na]^+$.

Synthesis of Carbamate-Protected Derivatives ***5a,p,b***. Compounds **4a,p,b** (48 mg, 0.1 mmol, 31 mg, 0.07 mmol, 73 mg, 0.14 mmol respectively) and TBAF solution (1.5 equiv for **4a,b** and 2.5 equiv for **4p**) were dissolved in anhydrous THF (3 mL) and stirred at room temperature for 3 h (for **5b**) or overnight (for **5a,p**). The resulting mixture was concentrated *in vacuo* and purified via flash chromatography (eluent: 6% MeOH in DCM) to yield compounds **5a,p,b** as white solids.

*4-(Allyloxycarbonylamino)-1-(2-deoxy-2,2-difluoro-β-D-erythro-pentofuranosyl)pyrimidin-2(1H)-one [**5a**]*. Thirty-two milligrams (92% yield). R_f 0.27 (10% MeOH in DCM). ^{1}H NMR (500 MHz, DMSO) δ 10.96 (s, 1H), 8.23 (d, *J* = 7.6, 1H), 7.10 (d, *J* = 7.6, 1H), 6.31 (d, *J* = 6.5, 1H), 6.16 (t, *J* = 7.5, 1H), 6.00−5.89 (m, 1H), 5.42−5.21 (m, 3H), 4.64 (d, *J* = 5.3, 2H), 4.24−4.13 (m, 1H), 3.88 (dt, *J* = 8.5, 3.1, 1H), 3.84−3.61 (m, 2H). ^{13}C NMR (126 MHz, DMSO) δ 163.40 (C), 153.99 (C), 152.82 (C), 144.45 (CH), 132.39 (CH), 122.94 (t, J_{C-F} = 258.3, C), 118.04 (CH_2), 94.82 (CH), 84.07 (t, J_{C-F} = 32.8, CH), 80.98 (CH), 68.37 (t, J_{C-F} = 22.7, CH), 65.64 (CH_2), 58.79 (CH_2). LRMS (ESI) *m*/*z* 346.0 $[M - H]^-$. HRMS (FAB) *m*/*z* $[M - H]^-$ calcd for $C_{13}H_{14}O_6N_3F_2$, 346.0856; found, 346.0853.

*4-(Propargyloxycarbonylamino)-1-(2-deoxy-2,2-difluoro-β-D-erythro-pentofuranosyl)pyrimidin-2(1H)-one (**5p**)*. Fifteen milligrams (62% yield). R_f 0.41 (10% MeOH in DCM). ^{1}H NMR (500 MHz, DMSO) δ 11.06 (s, 1H), 8.25 (d, *J* = 7.6, 1H), 7.08 (d, *J* = 7.6, 1H), 6.30 (d, *J* = 6.5, 1H), 6.16 (t, *J* = 7.4, 1H), 5.29 (t, *J* = 5.4, 1H), 4.80 (d, *J* = 2.3, 2H), 4.25−4.13 (m, 1H), 3.89 (dt, *J* = 8.5, 3.1, 1H), 3.84−3.63 (m, 2H), 3.62 (t, *J* = 2.3, 1H). ^{13}C NMR (126 MHz, DMSO) δ 163.26 (C), 153.93 (C), 152.37 (C), 144.61 (CH), 122.92 (C), 94.80 (CH), 84.09 (CH), 81.01 (CH), 78.21 (CH), 78.18 (C) 68.37 (CH), 58.78 (CH_2), 53.01 (CH_2). LRMS (ESI) *m*/*z* 344.0 $[M - H]^-$. HRMS (FAB) *m*/*z* $[M - H]^-$ calcd for $C_{13}H_{12}O_6N_3F_2$, 344.0700; found, 344.0719.

*4-(Benzyloxycarbonylamino)-1-(2-deoxy-2,2-difluoro-β-D-erythro-pentofuranosyl)pyrimidin-2(1H)-one (**5b**)*. Fifty-one milligrams, 92% yield. R_f 0.42 (10% MeOH in DCM). ^{1}H NMR (500 MHz, DMSO) δ 10.98 (s, 1H), 8.23 (d, *J* = 7.6, 1H), 7.45−7.32 (m, 5H), 7.11 (d, *J* = 7.6, 1H), 6.31 (d, *J* = 6.5, 1H), 6.16 (t, *J* = 7.4, 1H), 5.29 (t, *J* = 5.5, 1H), 5.20 (s, 2H), 4.25−4.13 (m, 1H), 3.88 (dt, *J* = 8.5, 3.1, 1H), 3.84−3.62 (m, 2H). ^{13}C NMR (126 MHz, DMSO) δ 163.38 (C), 153.99 (C), 153.00 (C), 144.46 (CH), 135.81 (C), 128.48 (CH_2), 128.19 (CH), 127.96 (CH_2), 122.93 (t, J_{C-F} = 259.6, C), 94.86 (CH), 84.08 (t, J_{C-F} = 30.2, CH), 80.98 (CH), 68.37 (t, J_{C-F} = 22.7, CH), 66.67 (CH_2), 58.78 (CH_2). LRMS (ESI) *m*/*z* 396.1 $[M - H]^-$. HRMS (FAB) *m*/*z* $[M - H]^-$ calcd for $C_{17}H_{16}O_6N_3F_2$, 396.1013; found, 396.1016.

Synthesis of Nonfluorescent Probes ***8a,p***. Probes **8a**[14] and **8p**[8] were prepared from rhodamine 110 chloride, **7**, as previously described.[14,8]

Synthesis of Nonfluorescent Probe ***8b***. Under a nitrogen atmosphere, rhodamine 110 chloride (150 mg, 0.41 mmol) was dissolved in dry DMF (4 mL). Separately, benzyl chloroformate (350 μL, 2.45 mmol) and pyridine (298 μL, 3.69 mmol) were dissolved in DMF (1 mL) and added dropwise to the mixture. The reaction mixture was stirred at r.t. for 48 h, solvents removed *in vacuo*, and the resulting crude resuspended in 25% isopropanol in $CHCl_3$ (30 mL) and washed with H_2O. The aqueous layer was then washed 5 times with 25% isopropanol in $CHCl_3$ (30 mL). The combined organic layers were dried over anhydrous $MgSO_4$ and the solids filtered off and concentrated *in vacuo*. The crude was purified via flash chromatography (hexane/ethyl acetate 2:1) to yield bis-*N*,*N*′-benzyloxycarbonyl-rhodamine 110 (**8b**) as a white solid (31 mg, 13%). R_f 0.23 (hexane/ethyl acetate 2:1); ^{1}H NMR (500 MHz, DMSO) δ 10.12 (s, 2H), 8.01 (d, *J* = 7.6, 1H), 7.78 (t, *J* = 7.1, 1H), 7.72 (t, *J* = 7.3, 1H), 7.58 (d, *J* = 1.7, 2H), 7.45−7.33 (m, 10H), 7.27 (d, *J* = 7.6, 1H), 7.20−7.12 (m, 2H), 6.70 (d, *J* = 8.7, 2H), 5.18 (s, 4H). ^{13}C NMR (126 MHz, DMSO) δ 168.66 (C), 153.25 (C)$_2$, 152.51 (C)$_2$, 150.94 (C), 141.43 (C)$_2$, 136.31 (C)$_2$, 135.71 (CH), 130.21 (CH), 128.53 (CH)2, 128.47 (CH)4 128.19 (CH_4), 128.14 (CH)2 125.71 (C), 124.77 (CH), 123.95 (CH), 114.46 (CH_2), 112.48 (C)$_2$, 105.10 (CH_2), 81.94 (C), 66.07 (CH_2)$_2$. MS (ESI) *m*/*z* 597.2 $[M - H]^-$.

Biological Studies. *General Methods.* Cell lines were grown in culture media supplemented with serum (10% FBS) and L-glutamine (2 mM) and incubated in a tissue culture incubator at 37 °C and 5% CO_2. Human pancreas adenocarcinoma BxPC-3 cells (a kind gift from Dr. Mark Duxbury) were cultured in Roswell Park Memorial Institute (RPMI) media. Human pancreatic carcinoma Mia PaCa-2 cells (a kind gift from Dr. Simon Wilkinson) were cultured in Dulbecco's modified Eagle's media (DMEM).

Cell Viability Studies. Cells were seeded in a 96 well plate format at the appropriate cell concentration (2,500 cells/well for BxPC-3 cells and 1,000 cells/well for MiaPaCa-2 cells) and incubated for 48 h before treatment. Each well was then replaced with fresh media containing compound **1** or **2a,p,b**/**5a,p,b** and incubated for 4 days. Untreated cells were incubated with DMSO (0.1% v/v). PrestoBlue

cell viability reagent (10% v/v) was added to each well and the plate incubated for 1 h. Fluorescence emission was detected using a PerkinElmer Victor^2 multilabel reader (excitation filter at 540 nm and emissions filter at 590 nm). All conditions were normalized to the untreated cells (100%) and curves fitted using GraphPad Prism using a sigmoidal variable slope curve.

*Pd^0-Mediated Deprotection of **5a,p,b** in Biocompatible Conditions.* Compounds **5a**, **5p**, and **5b** (100 μM) were dissolved in PBS (1 mL) with 1 mg of Pd^0-resins and shaken at 1400 rpm and 37 °C in a Thermomixer. Reaction crudes were monitored at 0, 6, 24, and 48 h by analytical HPLC (Agilent) using an UV detector at 280 nm to avoid the detection of PBS salts. Eluent A, water and formic acid (0.1%); eluent B, acetonitrile and formic acid (0.1%); A/B = 95:5 to 5:95 in 3 min, isocratic 1 min, 5:95 to 95:5 in 1 min, and isocratic 1 min.

*Pd^0-Mediated Dealkylation of **5a,p,b** in Cell Culture.* BxPC-3 and MiaPaCa-2 cells were plated as described before. Each well was then replaced with fresh media containing Pd^0-resins (0.67 mg/mL) with DMSO (0.1% v/v); **5a,p,b** (3, 10, 30, 100, and 300 nM) with DMSO (0.1% v/v); gemcitabine (3, 10, 30, 100, and 300 nM) with DMSO (0.1% v/v); or a combination of 0.67 mg/mL of Pd^0-resins + **5a,p,b** (3, 10, 30, 100, and 300 nM) with DMSO (0.1% v/v). Untreated cells were incubated with DMSO (0.1% v/v).

Cell Viability Assay. Cells were incubated with drugs for 5 days. PrestoBlue cell viability reagent (10% v/v) was added to each well and the plate incubated for 60 min. Fluorescence emission was detected and results normalized as described above.

Time-Lapse Imaging Study. BxPC-3 cell growth studies were carried out at a single dose of gemcitabine (1) or **5a,p** (30 nM). Each well was imaged every 3 h over 5 d under standard incubation conditions using an IncuCyte ZOOM microscope (placed inside the incubator). Image-based analysis of cell confluence and Supporting Information movie 1 were produced using the IncuCyte software.

DNA Damage Study. Mia PaCa-2 cells were seeded in an 8-well chamber slide with a density of 2,000 cells/well and incubated for 48 h prior to treatment. Each well was then replaced with fresh media containing 0.1% DMSO (v/v) and the following treatments: Pd^0-resins (0.67 mg/mL); **5p** (300 nM); **1** (300 nM); or a combination of Pd^0-resin + **5p** (300 nM). The combination of **5p** and Pd^0 resins were incubated for 24 h at 37 °C prior to treatment with cells. Following 24 h of treatment, cells were fixed with paraformaldehyde (4%, 20 min) and permeabilized cells (Triton X-100, 0.1%) subsequently treated with rabbit monoclonal antibody against Phospho-Histone H2AX (Ser139) (1:400, Cell Signaling Technologies, cat. no. 9718) for 1 h at room temperature. This was followed by 1 h of incubation at room temperature with secondary Alexa Fluor 488 linked antibody (1:1000, goat antirabbit, IgG, Life Technologies), Hoechst 33342 (1:8000, Life Technologies), and Alexa Fluor 594 Phalloidin (1:500, Life Technologies). Cells seeded in the chamber slide were imaged using an Olympus FV1000 microscope and merged using the ImageJ software (National Institutes of Health).

Zebrafish Studies. Wild type zebrafish embryos were collected from AB-TPL breeding pairs and reared at 28 °C in E3 embryo medium. Twenty-four hours postfertilization, embryos were treated with the anesthetic tricaine and pierced in the yolk with a fine needle. Either nonfunctionalized resin or a Pd^0-resin was then rapidly inserted into the yolk. Embryos that lost significant yolk in the procedure were removed from the experiment. Embryos were then gently transferred to fresh E3 medium and returned to 28 °C to ensure the yolk wound was closed. The corresponding probe (**8a,p,b**) was added to the embryo medium (final concentration 5 μM) and fish incubated for additional 24 h at 31 °C. Fish were imaged using fluorescent microscopy (Olympus Scan-R). The fold change in fluorescence with the Pd^0 resin + **8p** in comparison to that with the inactive resin + **8p** were quantified using ImageJ software. A line was drawn horizontally over the yolk sac of the embryo encompassing both the resin beads and the area surrounding them (Figure 8b,c), and the pixel intensities along the lines were calculated (Figure 8d). Experiments were repeated at least twice with n = 4/per condition. Zebrafish husbandry and experiments were performed under Home Office License in compliance with the Animals (Scientific Procedures) Act 1986 and approved by the University of Edinburgh Ethics Committee.

■ ASSOCIATED CONTENT

Ⓢ Supporting Information

NMR spectra of compounds **2a,p,b**, **5a,p,b**, and **8a,p,b** and 5-day time-lapse motion picture of pancreatic BxPC-3 cell proliferation under treatment with 30 nM **5a**; Pd^0-resins + 30 nM **5a**; 30 nM of **5p**; and Pd^0-resins + 30 nM of **5p**. This material is available free of charge via the Internet at http://pubs.acs.org.

■ AUTHOR INFORMATION

Corresponding Author

*Phone: 00 44 1317773584. E-mail: Asier.Unciti-Broceta@igmm.ed.ac.uk.

Notes

The opinions expressed in this publication are those of the authors and do not necessarily represent those of MSD, nor its affiliates.

The authors declare no competing financial interest.

■ ACKNOWLEDGMENTS

J.T.W. is grateful to the College of Medicine and Veterinary Medicine and the University of Edinburgh for a Darwin International Scholarship and an Edinburgh Global Research Scholarship. N.O.C. and A.U.B. thank RCUK and IGMM, respectively, for an Academic Fellowship. W.R., C.F., and E.E.P. are funded by the MRC. We are grateful to the Edinburgh Cancer Research UK Centre for funding this research through the CRUK Development Fund. This work has been partly funded by a Heriot Watt University − IGMM pilot project and the MSD Scottish Life Sciences Fund. We also thank Dr. Mark Duxbury for his helpful comments regarding the clinical applications of the prodrug approach.

■ ABBREVIATIONS USED

BOOM, bioorthogonal organometallic; Alloc, allyloxycarbonyl; Poc, propargyloxycarbonyl; Cbz, carboxybenzyl; TBS-Cl, *tert*-butyldimethylsilyl chloride; TBAF, tetrabutylammonium fluoride; dpf, days postfertilization; TLC, thin layer chromatography; DBU, 1,8-diazabicycloundec-7-ene; DMF, dimethylformamide; DCM, dichloromethane; r.t., room temperature; CD_3OD, deuterated methanol; RPMI, Roswell Park Memorial Institute; DMEM, Dulbecco's modified Eagle's media; DMSO, dimethyl sulfoxide

■ REFERENCES

(1) Sletten, E. M.; Bertozzi, C. R. Bioorthogonal chemistry: fishing for selectivity in a sea of functionality. *Angew. Chem. Int. Ed.* **2009**, *48*, 6974−6998.

(2) Ramil, C. P.; Lin, Q. Bioorthogonal chemistry: strategies and recent developments. *Chem. Commun.* **2013**, *49*, 11007−11022.

(3) Bertozzi, C. R. A decade of bioorthogonal chemistry. *Acc. Chem. Res.* **2011**, *44*, 651−653 and articles within the "Bioorthogonal Chemistry in Biology" special issue.

(4) Lang, K.; Chin, J. W. Bioorthogonal reactions for labeling proteins. *ACS Chem. Biol.* **2014**, *9*, 16−20.

(5) Castano, A. P.; Mroz, P.; Hamblin, M. R. Photodynamic therapy and anti-tumour immunity. *Nat. Rev. Cancer* **2006**, *6*, 535−545.

(6) Lim, R. K.; Lin, Q. Photoinducible bioorthogonal chemistry: a spatiotemporally controllable tool to visualize and perturb proteins in live cells. *Acc. Chem. Res.* **2011**, *44*, 828−839.

(7) Velema, W. A.; Szymanski, W.; Feringa, B. L. Photopharmacology: beyond proof of principle. *J. Am. Chem. Soc.* **2014**, *136*, 2178−2191.
(8) Weiss, J. T.; Dawson, J. C.; Macleod, K. G.; Rybski, W.; Fraser, C.; Torres-Sánchez, C.; Patton, E. E.; Bradley, M.; Carragher, N. O.; Unciti-Broceta, A. Extracellular palladium-catalysed dealkylation of 5-fluoro-1-propargyl-uracil as a bioorthogonally activated prodrug approach. *Nat. Commun.* **2014**, *5*, 3277.
(9) Saxon, E.; Bertozzi, C. R. Cell surface engineering by a modified Staudinger reaction. *Science* **2000**, *287*, 2007−2010.
(10) Agard, N. J.; Prescher, J.; Bertozzi, C. R. A strain-promoted [3 + 2] azide-alkyne cycloaddition for covalent modification of biomolecules in living systems. *J. Am. Chem. Soc.* **2004**, *126*, 15046−15047.
(11) Sletten, E. M.; Bertozzi, C. R. From mechanism to mouse: a tale of two bioorthogonal reactions. *Acc. Chem. Res.* **2011**, *44*, 666−676.
(12) Li, H.; Fan, J.; Peng, X. Colourimetric and fluorescent probes for the optical detection of palladium ions. *Chem. Soc. Rev.* **2013**, *42*, 7943−7962.
(13) Sasmal, P. K.; Streu, C. N.; Meggers, E. Metal complex catalysis in living biological systems. *Chem. Commun.* **2013**, *49*, 1581−1587.
(14) Unciti-Broceta, A.; Johansson, E. M. V.; Yusop, R. M.; Sánchez-Martín, R. M.; Bradley, M. Synthesis of polystyrene microspheres and functionalization with Pd(0) nanoparticles to perform bioorthogonal organometallic chemistry in living cells. *Nat. Protoc.* **2012**, *7*, 1207−1218.
(15) Salic, A.; Mitchison, T. J. A chemical method for fast and sensitive detection of DNA synthesis in vivo. *Proc. Natl. Acad. Sci. U.S.A.* **2008**, *105*, 2415−2420.
(16) Streu, C.; Meggers, E. Ruthenium-induced allylcarbamate cleavage in living cells. *Angew. Chem. Int. Ed.* **2006**, *45*, 5645−5648.
(17) Mascareñas, J. L.; Sánchez, M. I.; Penas, C.; Vázquez, M. E. Metal-catalyzed uncaging of DNA-binding agents in living cells. *Chem. Sci.* **2014**, *5*, 1901−1907.
(18) Sasmal, P. K.; Streu, C. N.; Meggers, E. Metal complex catalysis in living biological systems. *Chem. Commun.* **2013**, *49*, 1581−1587.
(19) Yusop, R. M.; Unciti-Broceta, A.; Johansson, E. M. V.; Sánchez-Martín, R. M.; Bradley, M. Palladium-mediated intracellular chemistry. *Nat. Chem.* **2011**, *3*, 239−243.
(20) Li, N.; Lim, R. K.; Edwardraja, S.; Lin, Q. Copper-free Sonogashira cross-coupling for functionalization of alkyne-encoded proteins in aqueous medium and in bacterial cells. *J. Am. Chem. Soc.* **2011**, *133*, 15316−15319.
(21) Spicer, C. D.; Triemer, T.; Davis, B. G. Palladium-mediated cell-surface labelling. *J. Am. Chem. Soc.* **2012**, *134*, 800−803.
(22) Michel, B. W.; Lippert, A. R.; Chang, C. J. A reaction-based fluorescent probe for selective imaging of carbon monoxide in living cells using a palladium-mediated carbonylation. *J. Am. Chem. Soc.* **2012**, *134*, 15668−15671.
(23) Spicer, C. D.; Davis, B. G. Rewriting the bacterial glycocalyx via Suzuki-Miyaura cross-coupling. *Chem. Commun.* **2013**, *49*, 2747−2749.
(24) Eli Lilly and Company. Gemzar (Gemcitabine) Prescribing Information. http://pi.lilly.com/us/gemzar.pdf.
(25) Rahma, O. E.; Duffy, A.; Liewehr, D. J.; Steinberg, S. M.; Greten, T. F. Second-line treatment in advanced pancreatic cancer: a comprehensive analysis of published clinical trials. *Ann. Oncol.* **2013**, *24*, 1972−1979.
(26) Cerqueira, N. M. F. S. A.; Fernández, P. A.; Ramos, M. J. Understanding ribonucleotide reductase inactivation by gemcitabine. *Chem.—Eur. J.* **2007**, *13*, 8507−8515.
(27) Hazra, S.; Ort, S.; Konra, M.; Lavie, A. Structural and kinetic characterization of human deoxycytidine kinase variants able to phosphorylate 5-substituted deoxycytidine and thymidine analogues. *Biochemistry* **2010**, *49*, 6784−6790.
(28) Ciccolini, J.; Mercier, C.; Dahan, L.; André, N. Integrating pharmacogenetics into gemcitabine dosing-time for a change? *Nat. Rev. Clin. Oncol.* **2011**, *8*, 439−444.
(29) Kocienski, P. J. In *Protecting Groups*; Georg Thieme: Stuttgart, Germany, 1994; and references therein.
(30) Guibé, F. Allylic protecting groups and their use in a complex environment part II: Allylic protecting groups and their removal through catalytic palladium π-allyl methodology. *Tetrahedron* **1998**, *54*, 2967−3042.
(31) Jarowicki, K.; Kocienski, P. Protecting groups. *J. Chem. Soc., Perkin Trans. 1* **2001**, 2109−2135.
(32) Ramesh, R.; Bhat, R. G.; Chandrasekaran, S. Highly selective deblocking of propargyl carbonates in the presence of propargyl carbamates with tetrathiomolybdate. *J. Org. Chem.* **2005**, *70*, 837−840.
(33) Papageorgiou, E. A.; Gaunt, M. J.; Yu, J.-Q.; Spencer, J. B. Selective hydrogenolysis of novel benzyl carbamate protecting groups. *Org. Lett.* **2000**, *2*, 1049−1051.
(34) Sanchez-Martin, R. M.; Muzerelle, M.; Chitkul, N.; How, S. E.; Mittoo, S.; Bradley, M. Bead-based cellular analysis, sorting and multiplexing. *ChemBioChem* **2005**, *6*, 1341−1345.
(35) Unciti-Broceta, A.; Díaz-Mochón, J. J.; Sánchez-Martín, R. M.; Bradley, M. The use of solid supports to generate nucleic acid carriers. *Acc. Chem. Res.* **2011**, *45*, 1140−1152.
(36) Dhaliwal, K.; Alexander, L.; Escher, G.; Unciti-Broceta, A.; Jansen, M.; Mcdonald, N.; Cardenas-Maestre, J. M.; Sanchez-Martin, R.; Simpson, J.; Haslett, C.; Bradley, M. Multi-modal molecular imaging approaches to detect primary cells in preclinical models. *Faraday Discuss.* **2011**, *149*, 107−114.
(37) Santra, M.; Ko, S.-K.; Shin, I.; Ahnz, K. H. Fluorescent detection of palladium species with an O-propargylated fluorescein. *Chem. Commun.* **2010**, 3964−3966.
(38) Liu, B.; Wang, H.; Wang, T.; Bao, Y.; Du, F.; Tian, J.; Li, Q.; Bai, R. A new ratiometric ESIPT sensor for detection of palladium species in aqueous solution. *Chem. Commun.* **2012**, *48*, 2867−2869.
(39) Rambabua, D.; Bhavani, S.; Swamy, N. K.; Rao, M. V. B.; Pal, M. Pd/C-mediated depropargylation of propargyl ethers/amines in water. *Tetrahedron Lett.* **2013**, *54*, 1169−1173.
(40) Kuo, L. J.; Yang, L. γ-H2AX − A novel biomarker for DNA double-strand breaks. *In Vivo* **2008**, *22*, 305−310.
(41) Ewald, B.; Sampath, D.; Plunkett, W. H2AX phosphorylation marks gemcitabine-induced stalled replication forks and their collapse upon S-phase checkpoint abrogation. *Mol. Cancer Ther.* **2007**, *6*, 1239−1248.
(42) Wang, Z.; Zheng, S.; Cai, J.; Wang, P.; Feng, J.; Yang, X.; Zhang, L.; Ji, M.; Wu, F.; He, N.; Wan, N. Fluorescent artificial enzyme-linked immunoassay system based on Pd/C nanocatalyst and fluorescent chemodosimeter. *Anal. Chem.* **2013**, *85*, 11602−11609.
(43) Sasmal, P. K.; Carregal-Romero, S.; Parak, W. J.; Meggers, E. Light-triggered ruthenium-catalyzed allylcarbamate cleavage in biological environments. *Organometallics* **2012**, *31*, 5968−5970.
(44) Wang, J.; Song, F.; Wang, J.; Peng, X. A near-infrared and ratiometric fluorescent chemosensor for palladium. *Analyst* **2013**, *138*, 3667−3672.
(45) Bielski, R.; Witczak, Z. Strategies for coupling molecular units if subsequent decoupling is required. *Chem. Rev.* **2013**, *113*, 2205−2224.
(46) Li, J.; Yu, J.; Zhao, J.; Wang, J.; Zheng, S.; Lin, S.; Chen, L.; Yang, M.; Jia, S.; Zhang, X.; Chen, P. R. Palladium-triggered deprotection chemistry for protein activation in living cells. *Nat. Chem.* **2014**, *6*, 352−361.